



Project:  
Wideband SAR Interferometry, ESA Contract: 21318/07/NL/HE

## Executive Summary

Written by: R. Brcic, M. Eineder, IMF-SV, DLR  
T. Nagler, F. Müller, ENVEO  
K. Papathanassiou, HR-RK, DLR

With contributions from the study team  
N. Adam, A. Parizzi, IMF-SV, DLR  
R. Metzиг, DFD-BI, DLR  
U. Steinbrecher, D. Schulze, HR-SS, DLR  
R. Schneider, M. J. Sanjuan Ferrer, HR-RK, DLR

Date: December 9<sup>th</sup> 2009



## 1 Description of Problem

Interferometric processing (InSAR) of coherently acquired microwave synthetic aperture radar (SAR) images is a powerful method to measure double differential ranges (between individual pixels and between two SAR images) with millimetric accuracy. The differential range measurement from different positions in space (cross track) is today commonly used to generate **Digital Elevation Models** (DEMs). Another unique application is **ground motion mapping** if the images are taken at different times (repeat pass). No comparable method exists to map the deformation of geophysical processes with high resolution and accuracy.

All interferometric methods in use today are constrained by a severe limitation: Shifts larger than half a wavelength of typically 3–20 cm cause phase cycle ambiguities that need to be resolved. This process is called **phase unwrapping** (PU) or **absolute phase determination**. It is underdetermined and therefore the most challenging processing step in InSAR. Existing solutions are typically tailored to the individual problem using model assumptions such as a smooth terrain surface or constant motion velocity. Today's high bandwidth SAR systems approach the wavelength dimension with their range resolution. In this study we therefore investigate if correlation techniques can achieve wavelength accuracy and be used to support **single pixel PU without the use of models**.

Other severe error sources in repeat pass InSAR are changes in the earth's ionosphere and the troposphere due to varying Total Electron Content (TEC) and water vapor respectively. In order to differentiate these errors from algorithmic or SAR instrument errors our experiments are accompanied by theoretical analysis of the expected **propagation errors** and by careful assessment of the **meteorological situation** at the test sites during the time of image acquisition.

One problem specific to deformation mapping is phase decorrelation with time because of natural surface changes. The Persistent Scatterer Interferometry (PSI) method tackles this problem in using only selected stable points. Different methods exist to find these points by temporal or spatial analysis. In the study we test a new algorithm that uses **spatial spectral correlation properties**, the **Coherent Scatterer** (CS) method.

## 2 Datasets

During the course of this study, approximately 90 TerraSAR-X datatakes were acquired with about half being used for DEM generation and half for PSI as listed in Table 2-1.

Acquisitions for DEM generation were of two south American salt seas surrounded by mountains regions. The desert climate provided stable conditions which minimized atmospheric disturbances and ground changes while the combination of flat salt seas and rugged mountains allowed a thorough evaluation of the technique in extreme cases.

Acquisitions for PSI were of urban areas where many artificial PSs exist. For the primary test site of Paris, an interferometric stack of 25 acquisitions was available.

Acquired Datasets													
Area, Designation	Mission	Datasets	Dataset Parameters										
			Centre Coordinates		Range	Chirp	Sensor Mode	Polarisation Mode	Polarisation Channels	Beam Pattern	Incidence Angle	Pass Direction	Look Direction
Latitude	Longitude	Bandwidth											
Salar de Uyuni, Custom Chirp	DEM-P	4	-20.04	-67.62	300 (2x37.5)	Custom				Spotlight	32	Asc	
Salar de Uyuni		15	-20.42	-67.63	150						31	Asc	
Salar de Uyuni, Full Length		2			150								Asc
Salar de Arizaro, South	DEM-B	6	-24.98	-67.70	100	Nominal	Stripmap	Single	HH	Stripmap	39	Asc	Right
Salar de Arizaro, South West		2	-25.01	-67.93	100						37	Asc	
Salar de Arizaro, North		5	-24.46	-67.84	100						39	Asc	
Salar de Arizaro, North Crossing Orbit		6	-24.49	-67.98	150						37	Desc	
Salar de Arizaro, South Crossing Orbit		2	-24.93	-67.67	100						49	Desc	
<b>DEM Datasets</b>		<b>38</b>											
Paris	PSI-P	25	48.86	2.29					HH		35	Asc	
Venice, spot_014	PSI-B	4	45.44	12.33					VV		23	Asc	
Venice, spot_046		4	45.44	12.33					VV		38	Asc	
Venice, spot_061		4	45.44	12.33	300	Nominal	High Resolution Spotlight	Single	VV	Spotlight	43	Desc	Right
Venice, spot_079		5	45.44	12.33					VV		49	Asc	
Venice, spot_094		5	45.44	12.33					VV		53	Desc	
Kimberley		2	-28.75	24.77					HH		29	Asc	
Kimberley, Custom Chirp		2			300 (2x37.5)	Custom							Asc
<b>PSI Datasets</b>		<b>49</b>											
<b>Datasets</b>		<b>87</b>											

Table 2-1: A summary of (selected) datasets acquired during this project.



### 3 Atmospheric Effects

The impact of the troposphere and ionosphere in terms of the induced interferometric phase delay caused by changes between acquisitions was evaluated.

#### 3.1 Tropospheric Effects

Tropospheric effects may be separated into 1) an almost spatially invariant component due to the atmospheric gases  $N_2$ ,  $O_2$  and  $CO_2$ , 2) a spatially variant component resulting from vertical stratification effects where a variable delay is induced by changes in relief combined with variations in the atmosphere's vertical structure 3) a highly spatially variant component due to PWV (Precipitable Water Vapour).

A processing system was developed which delivers estimates these effects using meteorological station measurements, NWP (Numerical Weather Prediction) models, radiosondes and PWV maps provided by MERIS (Medium Resolution Imaging Spectrometer) onboard ENVISAT and MODIS (Moderate Resolution Imaging Spectrometer) onboard the TERRA and ACQUA satellites.

Results confirm the highly variable contribution of the troposphere to the interferometric phase of up to several radians, mainly due to changes in atmospheric water content. Interferometric phase shifts due to variations in the atmosphere's vertical stratification were on the order of one cycle over a difference in elevation of 0.5 km. Qualitatively comparing the estimates with topographically flattened interferograms and atmospheric phase screens revealed a similar pattern in the phase gradients and magnitudes. Due to the coarse 1 km resolution of MODIS PWV products, small scale structures, especially in Paris, could not be resolved. A detailed comparison was not possible as the lifetime of the relevant atmospheric structures is less than the time difference between the acquisition of SAR and optical satellite data. A coincident acquisition of atmospheric measurements and SAR data is very important.

#### 3.2 Ionospheric Effects

The ionospheric TEC and its spatial and temporal variations in range and/or azimuth are associated with phase shifts in SAR data. The strength of the effects depends on the TEC level and the carrier frequency of the SAR system. At X-band (9.65GHz) the effects of the constant TEC layer can be almost neglected, although gradients in range and azimuth may occur depending on TEC level. For example, at 1 TECU, a change in elevation of 5 degrees causes a shift variation of less than 1 mm over range. Changes in TECU over azimuth of about 0.001 cycles/km can also occur, this corresponds to a gradient of 0.1 cycles over a scene of length of 100 km which may be measurable. Strong spatial TEC gradients greater than  $0.1 \text{ TECU/km}^{-1}$  may, at X-band, cause range shifts on the order of decimetres. Faraday Rotation is a result of the ionospheric birefringence induced by the Earth's geomagnetic field. Even at high solar activity, the Faraday rotation angles are on the order of a few degrees and can be neglected.

## 4 Digital Elevation Model Generation

For the generation of DEMs, two images are taken from different elevation angles providing an effective cross track baseline  $B_{\perp}$  as shown in Fig. 4-1. The images should be acquired at the same time (single-pass interferometry) in order to avoid severe phase distortions due to changes in the propagation medium. Such a simultaneous acquisition can be performed by using two antennas as done with some airborne systems and with the Shuttle Radar Topography Mission (SRTM). More flexibility with respect to baseline sizing will be offered in the near future by the TanDEM-X mission where the TerraSAR-X and TanDEM-X satellites will be coupled in a single-pass interferometric constellation.

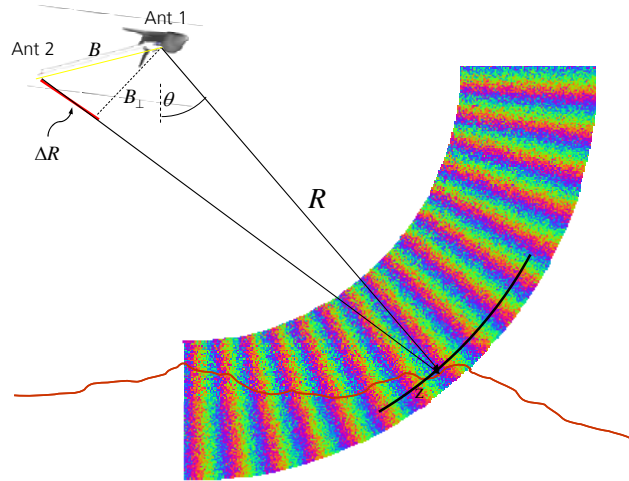


Fig. 4-1: Across track InSAR imaging configuration for DEM generation. The phase showed in cyclic colors is a noisy and ambiguous measure for the elevation angle of a pixel with a given range  $R$ .

All InSAR data processing systems for the aforementioned systems need to determine the unknown phase constant (cycle number) for each individual pixel. The problem is underdetermined meaning that no redundancy is available as for example in GPS processing, where multiple satellites allow bootstrapping algorithms to solve for the ambiguities. Conventional PU is performed by using at least one known control point from which phase gradients are estimated and then integrated over millions of pixels in the image. A single estimation error will then propagate over large areas resulting in at least one cycle ( $\lambda/2$ ) of error in the required range measurement. This in turn leads to generally unacceptable DEM height errors. In the SRTM dataset these unreliable areas have been masked out as shown in Fig. 4-2.

Phase ambiguity resolution can be efficiently supported by multiple images with varying baseline, as planned for the TanDEM-X mission, or multiple SAR frequencies which is expensive and therefore generally not done.

The method followed in this study is to **exploit the small frequency variation** within the range bandwidth for **absolute phase determination and ambiguity resolution**. The feasibility depends on the relative frequency variation with respect to the radar carrier

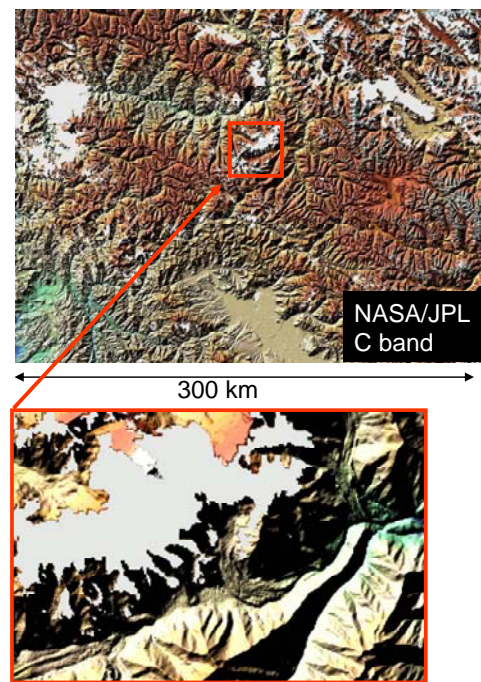


Fig. 4-2: Data voids in the SRTM DEM of the Himalayas due to unresolved PU problems.



frequency – the radar carrier frequency to bandwidth ratio – with **wideband interferometric systems** for which this parameter is small being most suitable. Table 4-1 lists this characteristic parameter for some past, current and future SAR systems. Due to data availability and suitability, this study focuses on TerraSAR-X data, however, the table shows a high potential for other current (PALSAR) and future (Sentinel-1) missions.

Satellite (Imaging Mode: StripMap, SpotLight)	Carrier Frequency $f_c$ [GHz] (Band)	Bandwidth B [MHz]	$\frac{f_c}{B}$	Typical Resolution [m]	Usability
TerraSAR-X (SM)	9.65 (X)	150	64	3 m	Good
TerraSAR-X (SL)	9.65 (X)	300	32	1 m	Very good
TanDEM-X (SM)	9.65 (X)	100	97	10 m	Moderate/good
Cosmo SkyMed (SM-SL)	9.65 (X)	65 – 400	24 – 148	1 – 3 m	Moderate/very good
Sentinel-1 (SM)	5.41 (C)	100	54	6 m	Good
RADARSAT-2	5.41 (C)	100	54	7 m	Good
PALSAR	1.27 (L)	28	45	7 m	Very good
Tandem-L/DESDynI (SM)	1.27 (L)	85	15	5 m	Excellent

Table 4-1: Carrier frequency to bandwidth ratio of current and future SAR missions with respect to wideband interferometry (a smaller ratio is better) and corresponding usability.

#### 4.1 Wideband DEM Generation

The delta-k technique for absolute phase estimation is to form a differential interferogram between two subband interferograms of bandwidth  $b$  obtained by bandpass filtering in range an interferometric pair of SAR images with bandwidth  $B$ . The delta-k phase can then be interpreted as the interferometric phase at a simulated carrier frequency  $B-b$ . The ratio  $f_c/(B-b)$  of the actual to simulated carrier frequencies corresponds to the increase in HoA (Height of Ambiguity) of the delta-k phase over the standard interferometric phase. For standard TerraSAR-X acquisitions with range bandwidth  $B = 150$  MHz and using subband bandwidths  $b = 50$  MHz, this factor is 64. Delta-k HoAs on the order of 1 km are then typical. Such a large HoA makes PU trivial or even unnecessary. The error in the delta-k absolute phase estimate is also increased by a factor approximately equal to the increase in HoA. This is compensated for by smoothing the delta-k phase. Delta-k is then a trade-off between resolution and the ability to resolve phase ambiguities due to the increase in HoA.

During our study **very good results** were achieved in all performed tests and even first applications of the delta-k method such as control of PU performance have been demonstrated – see the example in Fig. 4-3. A much wider range of operational applications, e.g. direct PU

support **should be investigated in the future**. This requires that the small residual trends that are still encountered are better understood and can be removed. Plausible error sources could be changes in the frequency dispersive ionosphere or changes in the frequency-phase response of the SAR instrument. An operational exploitation of this promising method would lead to stringent requirements on future SAR systems.

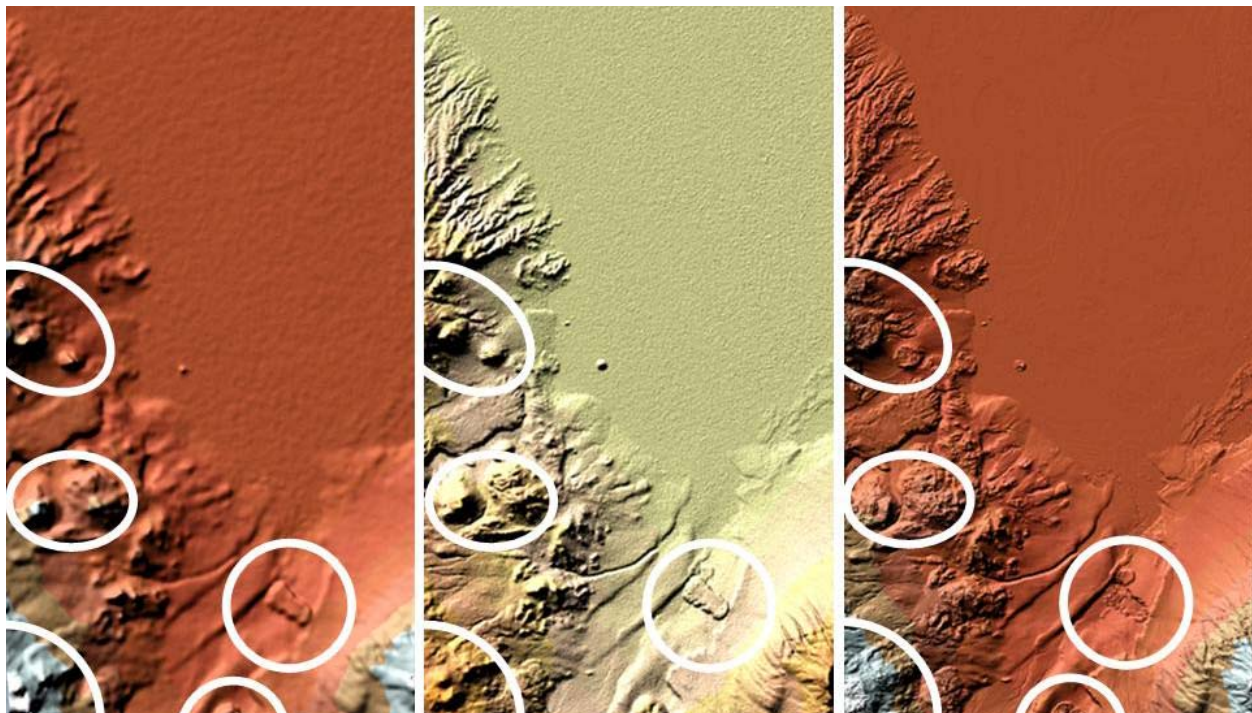


Fig. 4-3: DEM generation over the notoriously difficult salt sea Salar de Arizaro. Left: Correct DEM from delta-k absolute phase estimation. Middle: Correct SRTM C-band DEM. Right: Incorrect DEM from conventional PU. White circles denote obvious gross errors in the conventional estimate which were correctly recovered using delta-k.

The study also considered important questions such as the use of multiple subbands, optimal choice of subband bandwidth and use of custom split bandwidth chirps. The latter improves SNR by concentrating all transmitted energy in the subbands leading to a substantial increase in performance. During this study, a custom split bandwidth waveform was developed, uplinked to TSX-1 and used for SAR imaging for the first time – we are not aware of another experiment having used this technique before. Split bandwidth **custom chirps brought about a significant improvement** as predicted by theory. In this case the SNR was increased by 6 dB compared o a standard acquisition. Furthermore, given the appropriate hardware for bandpass filtering and subsampling of custom chirp acquisitions onboard the satellite, downlink bandwidth can be reduced to that required by the subbands.

## 5 Permanent Scatter Interferometry

Ground deformation imaging from space is an InSAR domain that is currently unmatched by any other technique. Fig. 5-1 demonstrates the principle of PSI. The double range difference between points  $P_1$  and  $P_2$  in the images taken at times  $t_1$  and  $t_2$  is measured by the ambiguous interferometric phase. In this difference phase wrapping can occur due to 1) fast motion  $\Delta R$ , 2) large height differences  $\Delta z$  if the baseline is not zero or 3) large differential propagation delays if the points are spatially separated by more than few hundred meters.

Due to the sparse sampling the PU problem is more complicated than for DEM generation but the PSI method seems to be a very good solution if time series of more than 20 images are available. In these image stacks, points are selected with preferably small distance and height differences. The amplitude stability versus time measured by the amplitude dispersion index is often used as a robust selection criteria but as this requires the analysis of many images, spatial or mixed spatio-temporal approaches are of interest. In this study we test a rather new algorithm, the **Coherent Scatterer selection method**.

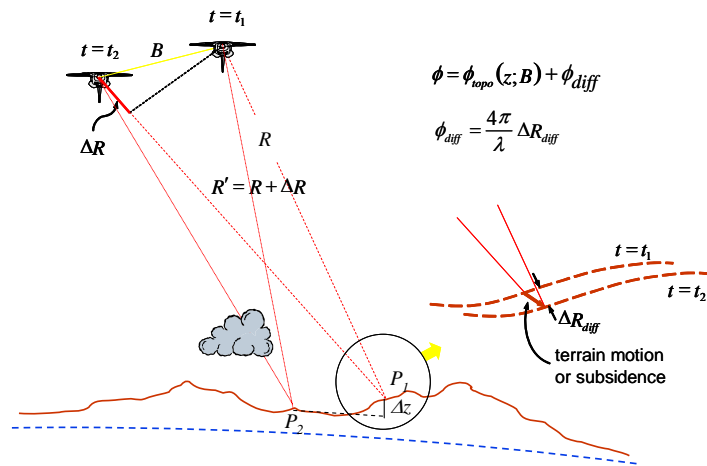


Fig. 5-1: PSI deformation measurement configuration from space. Phase wraps may be caused by large (fast) displacement  $\Delta R$ , by large height differences  $\Delta z$  or by atmospheric propagation delays.

The standard PSI method performs PU by fitting for each pixel a two-dimensional plane to the measured phase as a function of baseline and time – the so called ILS (Integer Least Squares) and periodogram techniques. This method was a breakthrough after its publication and proved both powerful and accurate as long as 1) the motion model is known and simple, e.g. linear and 2) the points are dense enough to avoid atmospheric and topographic phase wraps. These conditions are often fulfilled in cities but are not in many other locations and situations such as for volcano monitoring where non-linear motion occurs over large height differences and natural persistent scatterers are sparsely distributed.

**Having a reliable absolute phase determination technique would significantly improve the processing results of such areas. Fewer datasets would be required since the two dimensional phase fit to baseline and time would no longer be required.**

### 5.1 Wideband Persistent Scatterer Interferometry

A theoretical analysis of delta-k absolute phase estimation for a single PS showed that for TerraSAR-X 300 MHz high resolution spotlight acquisitions, an SCNR (Signal to Clutter and Noise Ratio) of approximately 33 dB is required in order to estimate the phase cycle ambiguity at the carrier frequency. In this case delta-k would provide a direct check of conventional estimates.

If it was found that for stable PSs with high SCNR and suitable HoAs, it is possible to determine the absolute phase or height using delta-k and avoid the error propagation which occurs in conventional sparse PU of PSI networks – see the example in Fig. 5-2. While achieving an accuracy on the order of one phase cycle at the carrier frequency proved difficult with current bandwidths, there is a great potential for delta-k techniques in PSI if larger bandwidths are used.

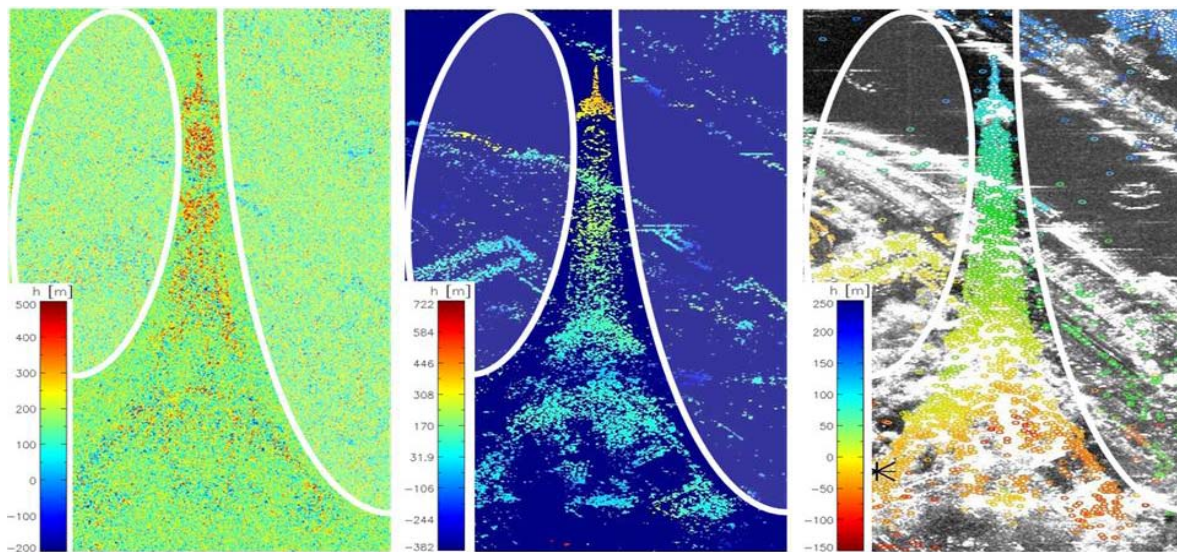


Fig. 5-2: Absolute phase estimation around the Eiffel tower – only relative heights between points are meaningful here. Left & Middle: Two types of delta-k estimates. Right: Conventional sparse PU estimate. White circles denote areas where conventional sparse PU failed and delta-k gave correct estimates.

## 5.2 Wideband Detection of Coherent Scatterers

An important class of scatterers in SAR images are point like scatterers. Their deterministic scattering behaviour combined with a characteristically high SNR makes them valuable for a wide spectrum of applications ranging from image calibration to object characterisation and information extraction. In the absence of speckle, their deterministic phase information is especially important with key applications in coherent SAR. CSs (Coherent Scatterers) are an important subclass of point scatterers characterised by stable spectral correlation. The advantage of CSs compared to other point scatterers is that they can be detected from a single SAR image. This allows a higher temporal resolution than conventional techniques.

Two major approaches to wideband CS (coherent scatterer) detection were considered, a sublook coherence detector based on the cross-correlation of two spectral subbands and a phase variance detector which better preserves spatial resolution. Both require only a single SAR acquisition in order to detect CSs. In order to do this they trade-off spatial resolution and the quality of the detected CSs in terms of SCR. For the phase variance approach, detection can be performed in both range and azimuth which improves the quality of the detected CSs.



## 6 Software

Prototype software which implements the delta-k technique for both DEM generation and PSI was developed and delivered to ESA. This was accompanied with a selection of datasets used in the study for testing purposes.

## 7 Conclusions and Recommendations

This study has advanced the field of (wideband) interferometry in several ways.

- Atmospheric effects were analysed and accurately predicted using a simulator which combined information from several meteorological sources.
- For DEM generation, the delta-k technique was demonstrated to be a much more robust way to estimate absolute phase than conventional PU of standard interferograms. In what is probably a first, custom split bandwidth chirp acquisitions were performed and used to generate a DEM.
- For PSI, the theoretical and experimental limits of delta-k absolute phase estimation were examined. First results show that absolute phase estimation for a single PS is possible and that with ever increasing system bandwidths, wideband techniques can only become more practical. It was also demonstrated that using only a single SAR image, it is possible to detect coherent scatterers which, due to their high SNR, provide information useful in object characterisation and calibration.

With a view to future missions, the performance of wideband techniques can be improved by 1) increasing the SNR or 2) reducing the carrier frequency to bandwidth ratio through increased range bandwidth or lower carrier frequency. From Table 4-1, the lowest carrier frequency to bandwidth ratio achievable with TerraSAR-X is 32. For the planned TanDEM-L / DESDyni mission this ratio drops to 15. For both the purposes of DEM generation and PSI, an increase in bandwidth is recommended to improve the performance of wideband absolute phase estimation. For DEM generation, performance is limited by SNR and hence custom chirps can be used to substantially improve performance. Furthermore, given the required onboard hardware, this can be achieved while at the same time substantially reducing downlink bandwidth. Hence, it is recommended that for the purposes of DEM generation, the use of custom chirps and the inclusion of necessary hardware onboard the satellite should be a consideration for future missions.